PHYSICAL REVIEW A VOLUME 35, NUMBER 4 FEBRUARY 15, 1987

Theory of quantum beats in optical transmission-correlation and pump-probe measurements

Masaharu Mitsunaga
NTT Electrical Communications Laboratories, Nippon Telegraph and Telephone Corporation, Musashino-shi, Tokyo 180, Japan

C. L. Tang
Cornell University, Ithaca, New York 14853

(Received 14 October 1986)

A full density-matrix theory for quantum beats in optical transmission-correlation or pump-probe type of experiments is developed. The model used is a three-level system with split excited-state levels. It is demonstrated on the basis of perturbation theory that quantum beats should be observable in such experiments. Theoretical and numerical results are compared with the complex details, including damped sinusoidal decays, observed in recent femtosecond relaxation studies of large organic dye molecules. It is also shown that there is no separately identifiable decay component corresponding to any homogeneous or inhomogeneous optical dephasing time in such experiments. Similar beating should also be observable in ultrafast spectroscopy using incoherent light and in Raman-type energy-level configurations where the ground state contains split levels.

I. INTRODUCTION

Recent femtosecond transmission-correlation[1] and pump-probe[2] studies of various organic dye molecules revealed surprising details in the relaxation dynamics of such large molecules. In addition to previously known picosecond processes, observations of initial exponential decays faster than 100 fsec and damped sinusoidal oscillations with a period on the order of 150 fsec were reported. It was suggested[1] that these damped oscillations might possibly represent quantum beats. The subject of quantum beats in the fluorescent light emitted by an atom[3] or a molecule[4] prepared in a coherent superposition of states by a pulse excitation has a long history,[5] and the theoretical basis for the effect is well established. In conventional quantum-beat experiments,[6] the fluorescence emitted is directly detected and the quantum beats show up as modulations superimposed on the exponential decay. The fastest beat that can be observed this way is generally on the order of 150 psec,[4] limited by the response time of the detection system. The conjecture that quantum beats on a femtosecond time scale could be seen in simple optical transmission type of experiments involving molecules suggests the need to demonstrate theoretically that this is indeed possible in principle. A detailed theory of quantum beats in transmission-correlation or pump-probe type of measurements is developed in this paper which takes full account of the effect of finite homogeneous relaxation rate T_2^{-1} and inhomogeneous broadening for the optical transitions. It shows that, as a general technique for observing quantum beats and measuring the corresponding homogeneous relaxation rate $T_{2\text{sub}}^{-1}$ for the sublevels in the excited and ground-state manifolds involved in the optical transitions, the transmission-correlation[7] or pump-probe[8] type of techniques offer an alternative to the conventional fluorescence type of measurements or other techniques such as those based upon photon-echoes[9,10] or polarization spectroscopy.[11,12]

The model we consider is a three-level system as shown schematically in Fig. 1. The excited state is assumed to consist of two sublevels 2 and 3. Optical transitions from the ground-state level 1 to both levels 2 and 3 are allowed. The system is initially prepared by a short optical pulse with a coherence width wider than the transition frequency ν_{32} and spans the split states $|2\rangle$ and $|3\rangle$. In conventional fluorescence-type quantum-beat experiments, the fluorescent light emitted after this initial pulse excitation is detected directly. The fluorescence decay is limited by the population relaxation time T_1 for the optical transitions $3\rightarrow 1$ and $2\rightarrow 1$. If the relaxation time $T_{2\text{sub}}$ for the "atomic coherence" between the sublevels 2 and 3 is long compared with the excitation pulse width τ_p and the oscillation period corresponding to the sublevel splitting ν_{32}, the fluorescence will show a sinusoidal modulation at ν_{32} with a damping time $T_{2\text{sub}}$, which is the quantum beat. This type of quantum beat can be seen regardless of the extent of inhomogeneous broadening or the homogeneous relaxation rate T_2^{-1} for the optical transitions $3\rightarrow 1$ and $2\rightarrow 1$. Such a quantum-beat experiment allows one to

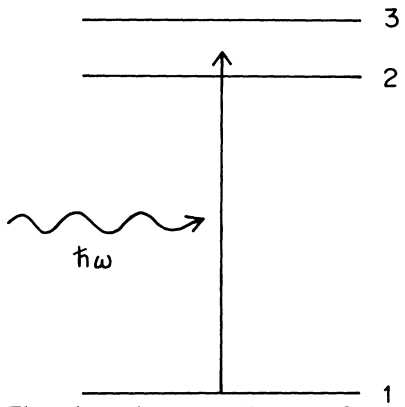

FIG. 1. The schematic energy diagram of a three-level system. The excited state consists of two sublevels 3 and 2.

measure the level splitting ν_{32} and the corresponding relaxation time $T_{2\text{sub}}$ in the presence of possibly very large optical-transition linewidths due to T_2 and the inhomogeneous broadening. However, because the beats are first measured as a transient feature on the fluorescence decay, the time resolution is limited by the response time of the detection system used to measure the fluorescence decay, which is typically in the picosecond to nanosecond range.

In the transmission-correlation or pump-probe type of experiments, the dynamics of the excited populations are probed by successively delayed short pulses with a pulse width shorter than all the dynamic features to be measured. More specifically, in the transmission-correlation type of experiments, for example, the sample is excited by two identical trains of repetitive ultrashort pulses with a variable delay τ between the two. The pulse repetition time τ_{rep} is generally long compared to all the transient features of interest but short compared to the integration time of the detection system. In the experiment both trains of pulses are sent collinearly through the sample to be measured. The time-averaged total transmitted power of both trains is measured as a function of the pulse delay τ. The measurement itself is basically a dc measurement and the response time of the detector is not a limitation. The quantum beats, if there are any, will show up in the measured transmitted power as a function of τ in the form of a damped sinusoidal oscillation $\sim e^{-|\tau|/T_{2\text{sub}}}\cos(\omega_{32}\tau)$ near zero delay, again regardless of the extent of homogeneous or inhomogeneous broadening of the optical transitions $3\rightarrow 1$ and $2\rightarrow 1$. The time resolution depends upon the pulse width and the resolution of the time delay between the two pulse trains. It is presently on the order of 10 fsec.

Physically, this type of quantum beat can be understood qualitatively as follows.[1] The first pulse at $t=0$ prepares the system in a coherent superposition of states as in the fluorescence-type quantum-beat experiments. Let this initial state at $t=0$ be

$$|a\rangle=\alpha|2\rangle+\beta|3\rangle ,$$

where α and β depend upon the optical transition moments between the states 1 and 2 and 1 and 3, and the energy of the first excitation pulse. At a later time $t=\tau$ larger than the pulse width τ_p, this coherent superposition state becomes

$$|a(\tau)\rangle=\alpha(\tau)e^{-(i/\hbar)E_2\tau}|2\rangle+\beta(\tau)e^{-(i/\hbar)E_3\tau}|3\rangle .$$

Projecting $|a(\tau)\rangle$ back onto $|a\rangle$ and with proper normalization gives the fraction of the excited-state population $|\langle a|a(\tau)\rangle|^2/|\langle a|a\rangle|^2$, that can be optically coupled to the ground state $|1\rangle$ at time τ. Through the saturation effect, the absorption or transmission of the delayed pulse at τ will be affected by the change in the rate of absorption, proportional to $|\langle a|a(\tau)\rangle|^2$, induced by the first pulse, which contains a modulation term

$$|\langle a|a(\tau)\rangle|^2_{\text{mod}}\propto\mathcal{R}\alpha(\tau)\beta^*(\tau)e^{i\omega_{32}\tau} .$$

Taking relaxation of the coherence between levels 2 and 3 into account, the statistically averaged $\overline{\alpha(\tau)\beta^*(\tau)}$ factor decays as $e^{-\tau/T_{2\text{sub}}}$. This leads to a damped sinusoidal modulation term in the absorption proportional to $e^{-\tau/T_{2\text{sub}}}\cos(\omega_{32}\tau)$. A full density-matrix treatment of this problem allowing for a finite pulse width, homogeneous optical relaxation rate T_2^{-1}, inhomogeneous broadening, population decay, and pulse overlap is developed in Sec. II for both the transmission-correlation and pump-probe types of experiments.

Quantum beats have also been seen in photon-echo or polarization-spectroscopy type of experiments.[9–12] In fact, Golub and Mossberg[13] have reported seeing beats at 140 fsec in Rb vapor using incoherent light. The key difference between the photon-echo type of experiments and those discussed in this paper is that quantum beats in the echo type of experiments can be seen only if the homogeneous relaxation rate T_2^{-1} for the optical transition is small compared to the beat frequency. There is no such restriction in the transmission-correlation or pump-probe type of experiments. The time-resolved polarization spectroscopy has been applied extensively to atomic systems in the nanosecond and picosecond time domains. The optical transmission-correlation and pump-probe experiments and the corresponding theory open the way for studying ultrafast molecular dynamics and femtosecond time-domain spectroscopy.

II. THEORY

A. General results

There are three main issues that need to be addressed beyond the simple considerations given in Sec. I. First, it must be shown that the beat signal is not masked by inhomogeneous broadening of the optical transitions 3-1 and 2-1. Second, whether the transmission-correlation or pump-probe type of measurements give any information on the homogeneous relaxation rate T_2^{-1} for the optical transitions. Third, it is well known that in such measurements there is a "coherent artifact"[8] contribution to the measured signal when the two pulses overlap. This coherent artifact significantly complicates[7,8] the interpretation of the data for relaxation processes on the order of or faster than the pulse width. Previous theories of this artifact all assumed infinitely fast dephasing time and no quantum beat. It is important to know how a finite T_2, inhomogeneous broadening, and level-splitting affect the coherent artifact. For these, a full density-matrix treatment is needed.

We consider the basic model shown in Fig. 1. As for the excitation, the envelope of the electric field is assumed for the moment to have an arbitrary shape. Later we consider the case of time-delayed two equal pulses. The equation of motion for the corresponding 3×3 density matrix is

$$\frac{d\rho}{dt}=\frac{i}{\hbar}[\rho,\mathcal{H}_0+\mathcal{H}_{\text{int}}]+(\text{decay term}) , \tag{1}$$

where

$$\mathcal{H}_0=\begin{bmatrix}\hbar\omega_{31} & 0 & 0\\ 0 & \hbar\omega_{21} & 0\\ 0 & 0 & 0\end{bmatrix} , \tag{2}$$

and

$$\mathscr{H}_{\text{int}} = -[\mathscr{E}(t)e^{-i\omega t} + \text{c.c.}] \begin{bmatrix} 0 & 0 & p_{31} \\ 0 & 0 & p_{21} \\ p_{13} & p_{12} & 0 \end{bmatrix} . \tag{3}$$

The dipole matrix elements p_{31} and p_{21} are both nonzero in general.

The decay term of Eq. (1) consists of four parts. The excited-state populations ρ_{33} and ρ_{22} decay with the same rate γ to other levels. The ground-state recovery time is much longer than the experimental time scale and can be neglected. The optical coherence components ρ_{31} and ρ_{21} relax with the rate T_2^{-1}, and the excited-state sublevel coherence component ρ_{32} decays with $T_{2\text{sub}}$. The decay terms, therefore, are summarized as

$$\begin{aligned} \left[\frac{d}{dt}\rho_{jj}\right]_{\text{decay}} &= -\gamma\rho_{jj}, \quad j=2,3 \\ \left[\frac{d}{dt}\rho_{11}\right]_{\text{decay}} &= 0 , \\ \left[\frac{d}{dt}\rho_{j1}\right]_{\text{decay}} &= -\rho_{j1}/T_2, \quad j=2,3 \\ \left[\frac{d}{dt}\rho_{32}\right]_{\text{decay}} &= -\rho_{32}/T_{2\text{sub}} . \end{aligned} \tag{4}$$

The pump-and-probe signal or the transmission-correlation signal will be calculated according to the following procedure. First, Eq. (1) is solved using the perturbation theory[14,15] for each component up to the third order. Next, the third-order solutions for the density-matrix elements are averaged over the inhomogeneous spectrum of the optical transition frequencies, which we assume to be Gaussian; for example,

$$g(\omega_{31}) = \frac{1}{2\sigma\sqrt{\pi}} e^{-(\omega_{31}-\omega)^2/4\sigma^2} . \tag{5}$$

The resulting third-order density-matrix elements $\rho_{31}^{(3)}$ and $\rho_{21}^{(3)}$ give the desired macroscopic polarization P,

$$\begin{aligned} P &= \text{Tr}(\rho p) \\ &= \rho_{31}p_{13} + \rho_{21}p_{12} + \text{c.c.} , \end{aligned} \tag{6}$$

which in turn gives the change in the transmitted power S through the medium

$$S = -\int dt\, \overline{E(t)\frac{d}{dt}P(t)} , \tag{7}$$

where the horizontal bar denotes time averaging over an optical cycle. Accordingly, the signal S is, from Eqs. (1)—(7),

$$\begin{aligned} S = &-\frac{2\omega\rho_0(|p_{31}|^2+|p_{21}|^2)}{\hbar}\mathscr{R}\int dt_2\int^{t_2} dt_1 \mathscr{E}^*(t_2)\mathscr{E}(t_1)e^{-(t_2-t_1)/T_2-\sigma^2(t_2-t_1)^2} \\ &+\frac{2\omega\rho_0}{\hbar^3}\mathscr{R}\int dt_4\int^{t_4} dt_3\int^{t_3} dt_2\int^{t_2} dt_1 e^{-(t_4-t_3+t_2-t_1)/T_2} \\ &\times\{\mathscr{E}^*(t_4)\mathscr{E}(t_3)\mathscr{E}^*(t_2)\mathscr{E}(t_1)(|p_{31}|^4+|p_{21}|^4) \\ &\quad\times e^{-\sigma^2(t_4-t_3+t_2-t_1)^2}(e^{-\gamma(t_3-t_2)}+1) \\ &+\mathscr{E}^*(t_4)\mathscr{E}(t_3)\mathscr{E}(t_2)\mathscr{E}^*(t_1)(|p_{31}|^4+|p_{21}|^4) \\ &\quad\times e^{-\sigma^2(t_4-t_3-t_2+t_1)^2}(e^{-\gamma(t_3-t_2)}+1) \\ &+2\mathscr{E}^*(t_4)\mathscr{E}(t_3)\mathscr{E}^*(t_2)\mathscr{E}(t_1)|p_{31}|^2|p_{21}|^2 e^{-\sigma^2(t_4-t_3+t_2-t_1)^2} \\ &\quad\times\cos[\omega_{32}(t_2-t_1)] \\ &+2\mathscr{E}^*(t_4)\mathscr{E}(t_3)\mathscr{E}(t_2)\mathscr{E}^*(t_1)|p_{31}|^2|p_{21}|^2 e^{-\sigma^2(t_4-t_3-t_2+t_1)^2} \\ &\quad\times\cos[\omega_{32}(t_2-t_1)] \\ &+2\mathscr{E}^*(t_4)\mathscr{E}(t_3)\mathscr{E}^*(t_2)\mathscr{E}(t_1)|p_{31}|^2|p_{21}|^2 \\ &\quad\times e^{-\sigma^2(t_4-t_3+t_2-t_1)^2-(t_3-t_2)/T_{2\text{sub}}}\cos[\omega_{32}(t_3-t_2)] \\ &+2\mathscr{E}^*(t_4)\mathscr{E}(t_3)\mathscr{E}(t_2)\mathscr{E}^*(t_1)|p_{31}|^2|p_{21}|^2 \\ &\quad\times e^{-\sigma^2(t_4-t_3-t_2+t_1)^2-(t_3-t_2)/T_{2\text{sub}}}\cos[\omega_{32}(t_3-t_1)]\} . \end{aligned} \tag{8}$$

The above expression gives the most general result for any arbitrary-shaped pulse excitation. The first term gives the linear absorption and the rest corresponds to the nonlinear absorption. Among the nonlinear absorption terms, the last two quantum-beat terms are of particular interest. In the following sections, this general result is analyzed for some specific cases.

B. Transmission-correlation measurement

We now consider specifically the transmission-correlation measurement which makes use of two pulses of equal amplitude, one delayed by τ from the other. The electric field envelope in this case is written as

$$\mathscr{E}(t)=\epsilon(t)+\epsilon(t-\tau)e^{i\omega\tau}\,, \tag{9}$$

where $\epsilon(t)$ is assumed to be real. The signal is obtained by substituting Eq. (9) into Eq. (8).

It should be emphasized here that the signal is analyzed as a function of the delay time τ. The terms which are independent of τ only gives a constant background and will be of no consequence and, hence, not considered further. Also notice the existence of the fringe terms.[16] If a term has an exponential factor corresponding to $e^{\pm i\omega\tau}$ or $e^{\pm 2i\omega\tau}$, it will oscillate very rapidly as τ is varied and will be averaged out to zero in the experiment; these terms should be neglected also. Following these considerations, the signal $S_{\rm TC}$ for the transmission-correlation measurement or the transmission-correlation peak (TCP) (Ref. 7) is derived from Eq. (9) as

$$\begin{aligned}S_{\rm TC}(\tau)=\frac{2\omega\rho_0}{\hbar^3}\int dt_4\int^{t_4}dt_3\int^{t_3}dt_2\int^{t_2}dt_1 e^{-(t_4-t_3+t_2-t_1)/T_2}&\\ \times[\epsilon(t_1)\epsilon(t_2)\epsilon(t_3-\tau)\epsilon(t_4-\tau)(N_++N_-+C_++C_-+B_++B_-)&\\ +\epsilon(t_1-\tau)\epsilon(t_2-\tau)\epsilon(t_3)\epsilon(t_4)(N_++N_-+C_++C_-+B_++B_-)&\\ +\epsilon(t_1)\epsilon(t_2-\tau)\epsilon(t_3-\tau)\epsilon(t_4)(N_++C_++B_+)&\\ +\epsilon(t_1-\tau)\epsilon(t_2)\epsilon(t_3)\epsilon(t_4-\tau)(N_++C_++B_+)&\\ +\epsilon(t_1)\epsilon(t_2-\tau)\epsilon(t_3)\epsilon(t_4-\tau)(N_-+C_-+B_-)&\\ +\epsilon(t_1-\tau)\epsilon(t_2)\epsilon(t_3-\tau)\epsilon(t_4)(N_-+C_-+B_-)]\,,&\end{aligned} \tag{10}$$

where

$$\begin{aligned}N_\pm&=(|p_{31}|^4+|p_{21}|^4)e^{-\sigma^2(t_4-t_3\pm t_2\mp t_1)^2}\\&\quad\times(e^{-\gamma(t_3-t_2)}+1)\,,\\C_\pm&=2|p_{31}|^2|p_{21}|^2e^{-\sigma^2(t_4-t_3\pm t_2\mp t_1)^2}\\&\quad\times\cos[\omega_{32}(t_2-t_1)]\,,\\B_+&=2|p_{31}|^2|p_{21}|^2e^{-\sigma^2(t_4-t_3+t_2-t_1)^2-(t_3-t_2)/T_{2\rm sub}}\\&\quad\times\cos[\omega_{32}(t_3-t_2)]\,,\\B_-&=2|p_{31}|^2|p_{21}|^2e^{-\sigma^2(t_4-t_3-t_2+t_1)^2-(t_3-t_2)/T_{2\rm sub}}\\&\quad\times\cos[\omega_{32}(t_3-t_1)]\,.\end{aligned} \tag{11}$$

The six terms of Eq. (10) are illustrated in Fig. 2. (Notice the time ordering $t_1<t_2<t_3<t_4$.) Each term is composed of simply decaying nonbeating components $N_\pm$, nondecaying components $C_\pm$, and, finally, beating components $B_\pm$. It is clear from the figure that the terms other than the first term disappear when the two pulses are well separated. Thus, the first term gives the most important contribution to the quantum-beat signal. On the

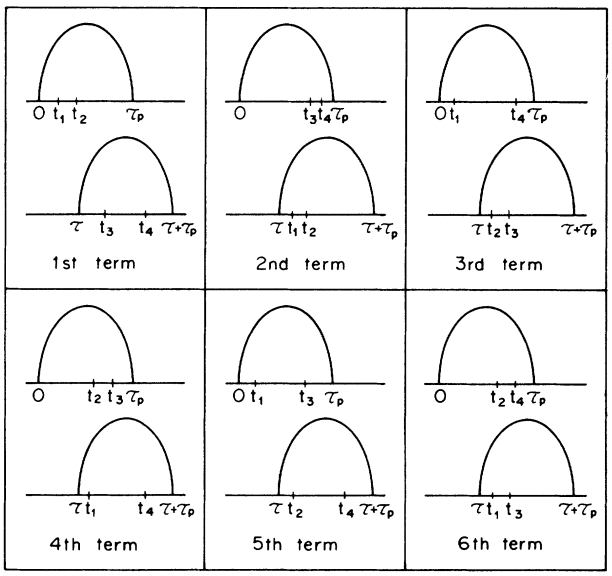

FIG. 2. Schematic illustration of the ordering of the time variables in Eq. (10). It should be emphasized that the time ordering is always $t_1<t_2<t_3<t_4$. τ is arbitrary. If $\tau>\tau_p$, terms 2—6 in the figure vanish. If $\tau<\tau_p$, all six terms are nonzero.

other hand, when the pulses overlap, all the terms become nonzero and produce the initial spike call coherent artifact.

Physically, the first term of Eq. (10) or Fig. 2 shows that the induced polarization P which leads to the absorption of the second (delayed) pulse is proportional to $P \propto E_1^2 E_2$, where E_1 and E_2 are the amplitudes of the first and the second pulses, respectively. The role of the first pulse is to create the excited-state population and the sublevel coherence, if there is any, and the decay $(\gamma^{-1}, T_{2\text{sub}})$ of these quantities is monitored by the second pulse as a function of the delay time τ, for τ larger than the pulse width τ_p.

There is an intrinsic difference between the transmission type of experiments as discussed here, and the photon-echo type of experiments, although both make use of a pair of short optical pulses and are due to the third-order nonlinear optical polarization $P \propto E^3$. In photon-echo experiments, the role of the first pulse is to create an optical coherence and its decay (T_2) is monitored as a function of τ. Therefore, the macroscopic polarization P, in this case, is proportional to $E_1 E_2^2$ instead of $E_1^2 E_2$. The echo is observed at a delay time on the order of or shorter than T_2. The behavior of Eq. (10) will be discussed in detail later.

C. Pump-probe measurement

In usual pump-probe experiments, the total electric field is given as

$$\mathscr{E}(t)=\epsilon(t)+\alpha_{\text{probe}}\epsilon(t-\tau)e^{i\omega\tau} , \tag{12}$$

where the coefficient α_{probe} is small compared to 1. The general result of Eq. (8) is slightly modified in this case because only the transmitted power of the probe beam, not both beams, is measured. This corresponds to including the probe field only in the $E(t)$ appearing in Eq. (7). Calculation similar to that in Sec. II B leads to

$$\begin{aligned} S_{\text{PP}}(\tau)=\frac{2\omega\rho_0\alpha_{\text{probe}}^2}{\hbar^3}\int dt_4\int^{t_4} dt_3\int^{t_3} dt_2\int^{t_2} dt_1 e^{-(t_4-t_3+t_2-t_1)/T_2} \\ \times[\epsilon(t_1)\epsilon(t_2)\epsilon(t_3-\tau)\epsilon(t_4-\tau)(N_+ +N_- +C_+ +C_- +B_+ +B_-) \\ +\epsilon(t_1-\tau)\epsilon(t_2)\epsilon(t_3)\epsilon(t_4-\tau)(N_+ +C_+ +B_+) \\ +\epsilon(t_1)\epsilon(t_2-\tau)\epsilon(t_3)\epsilon(t_4-\tau)(N_- +C_- +B_-)] , \end{aligned} \tag{13}$$

for the pump-probe signal $S_{\text{PP}}(\tau)$. We notice that the number of terms is reduced to a half in this case. For the special case where $\alpha_{\text{probe}}=1$, there is a very simple relationship between the transmission-correlation S_{TC} and the pump-probe S_{PP} signals:

$$S_{\text{TC}}(\tau)=S_{\text{PP}}(\tau)+S_{\text{PP}}(-\tau) . \tag{14}$$

This conclusion is rather natural since the transmission-correlation measurement is simply a symmetrized version of the pump-probe measurement with respect to the delay time τ.

D. Discussions

In this section, we discuss some special cases related to the transmission-correlation measurement [Eqs. (10) and (11)].

1. *Effect of pulsewidth*

One of the few examples where Eq. (10) can be evaluated analytically is the case when the pulse $\epsilon(t)$ is given by the delta function:

$$\epsilon(t)=\epsilon_0\delta(t) , \tag{15}$$

but the homogeneous or inhomogeneous optical dephasing time T_2 and T_2^* (determined from σ^{-1}) can be arbitrary. From Eq. (10) it is clear that in this case only the first term survives as the signal. The analytical solution in this case is

$$S_{\text{TC}}(\tau)\propto[(|p_{31}|^4+|p_{21}|^4)e^{-\gamma\tau} +2|p_{31}|^2|p_{21}|^2 e^{-\tau/T_{2\text{sub}}}\cos(\omega_{32}\tau)] . \tag{16}$$

This shows that the signal consists of two terms: the single exponential decay of rate γ, and the damped sinusoid with oscillation frequency ω_{32}. As might be expected, the optical dephasing times T_2 and T_2^* do not show up in the expression. The quantum-beat component becomes most pronounced when the two matrix elements $|p_{31}|$ and $|p_{21}|$ are equal.

For finite pulse widths, the integrals in Eq. (10) can be evaluated only numerically. We consider first the case when T_2 and T_2^* are equal to zero so that the finite pulse-length effect can be seen clearly. The corresponding signal lineshapes or the transmission-correlation peaks for different pulse widths are shown in Fig. 3. Here and henceforth we assume that the pulse shape is Gaussian. It can be seen that the main features remain the same, except that the oscillation amplitude is reduced as the pulse width exceeds the oscillation period. This is consistent with the experimental observation reported in Ref. 1.

2. *Effect of finite dephasing times T_2 and T_2^**

It is important to consider how optical dephasing times T_2 and T_2^* affect the signal line shape if they are intro-

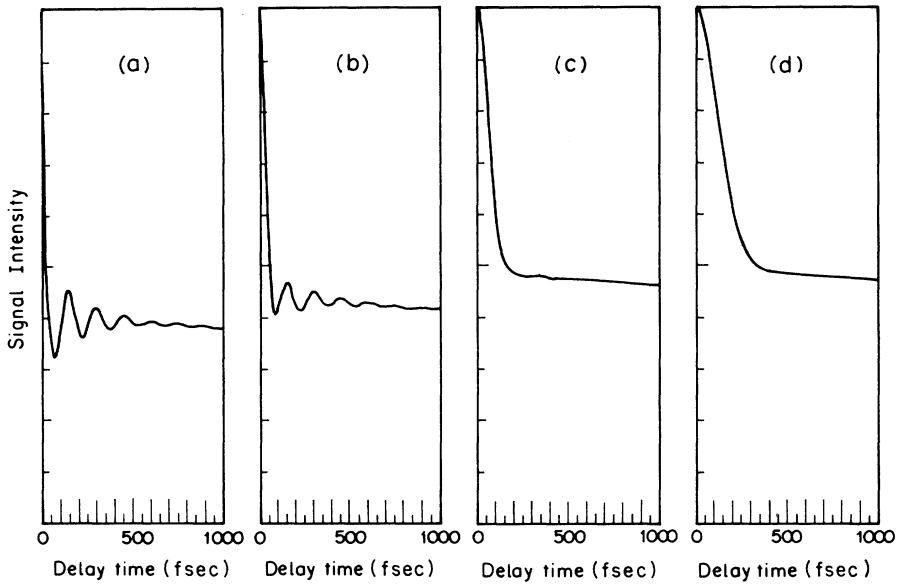

FIG. 3. Pulse-width (τ_p) dependence of transmission-correlation signal intensity. Equation (10) is numerically evaluated for $T_2=0$, $\gamma^{-1}=4.8$ psec, $T_{2\text{sub}}=190$ fsec, and $\nu_{32}^{-1}=150$ fsec. $|p_{31}|=|p_{21}|$. (a) $\tau_p=20$ fsec, (b) $\tau_p=50$ fsec, (c) $\tau_p=100$ fsec, (d) $\tau_p=200$ fsec.

duced into the theory, and to see if the signal line shape gives any information on T_2 or T_2^*.

The influence of T_2 and T_2^* can be qualitatively understood from Fig. 2 and Eq. (10). First consider the case of well-separated pulses, i.e., the first term of Fig. 2. The time variables t_1 and t_2 are chosen from the first pulse, while t_3 and t_4 are chosen from the second pulse. In the quadruple integrals of Eq. (10), the exponential factors which include T_2 or σ only depend on the time intervals between t_2 and t_1 and t_4 and t_3 but not on t_3 and t_2. On the other hand, the delay time τ is essentially given by the interval t_3 and t_2. Hence, if the signal is plotted as a function of τ, the information of the dephasing times should not show up at least when the pulses are well separated.

When T_2, T_2^*, and the pulse widths are finite, the gen-

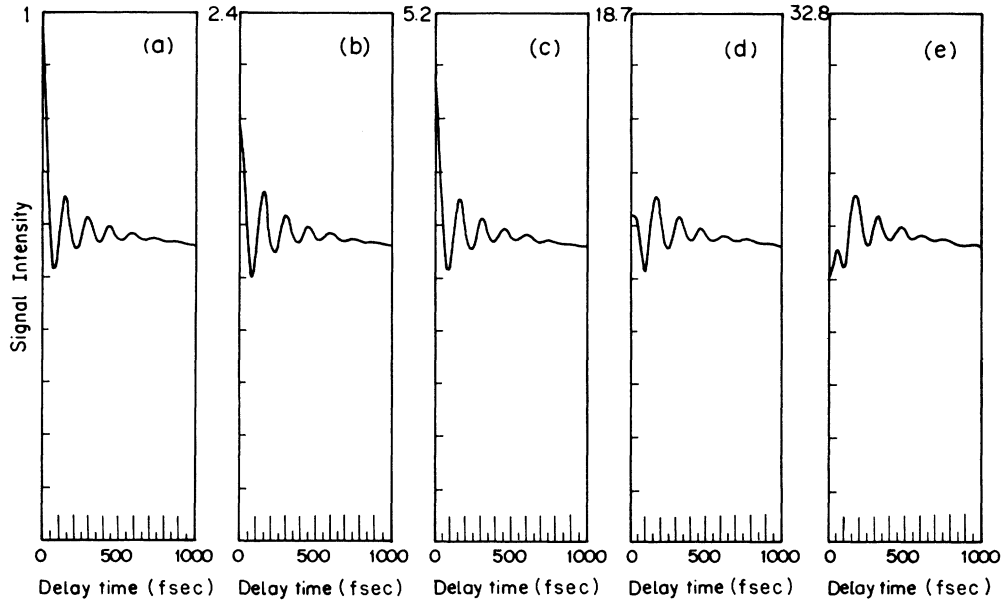

FIG. 4. Dephasing time (T_2, T_2^*) dependence of transmission-correlation signal intensity. Equation (10) is numerically evaluated for $\tau_p=40$ fsec, $\gamma^{-1}=4.8$ psec, $T_{2\text{sub}}=190$ fsec, and $\nu_{32}^{-1}=150$ fsec. $|p_{31}|=|p_{21}|$. (a) $T_2=20$ fsec, $T_2^*=6$ fsec, (b) $T_2=100$ fsec, $T_2^*=6$ fsec, (c) $T_2=20$ fsec, $T_2^*=100$ fsec, (d) $T_2=100$ fsec, $T_2^*=100$ fsec, and (e) $T_2=4.8$ psec, $T_2^*=10$ psec. Although the general patterns are similar, the magnitudes of the signal are very different. [Note the vertical scales of (a)—(e).]

eral problem is very complicated. Equation (10) can only be evaluated numerically. Various numerical examples obtained using a Cray computer are shown in Fig. 4. When two pulses overlap, the numerical results in Fig. 4 show that, generally, the magnitude of the coherent spike is higher for shorter dephasing times. For longer dephasing times, it is lower and the peak at $\tau=0$ may even become a dip instead of a peak for very long dephasing times. The shape of the quantum-beat signal and the width of the coherent spike region do not depend on the dephasing times, however. Thus, it is difficult to obtain any direct information on the values of T_2 or T_2^* from the signal line shape. Decay times γ^{-1} associated with the populations of some levels, the sublevel splitting ω_{32}, and coherence decay time $T_{2\text{sub}}$ are the principal information that can be obtained from the transmission-correlation type of experiments.

3. *Comparison with experiments*

In order to compare with the experimental result of Ref. 1, Eq. (10) is analyzed numerically using constants corresponding to the results for malachite green; that is, $\tau_p=40$ fsec, $\nu_{32}^{-1}=150$ fsec, $T_{2\text{sub}}=190$ fsec, $1/\gamma=4.8$ psec, and $1/\sigma=6$ fsec. The value of T_2 is unknown. However, according to the discussion given in Sec. II D 2, the signal line shape is relatively independent of T_2, except for the magnitude of the coherent spike. We arbitrarily assume T_2 to be 100 fsec. Reference 1 also reported a very fast relaxation component (60 fsec) in addition to the 150-fsec quantum beat and the slow (4.8-psec) population decay process. The previous discussion shows that this fast relaxation component cannot be due to any dephasing process. It is probably due to intramolecular population decay from photo-excited states not associated with those producing the quantum beats. In the numerical works, an additional decay channel with a relaxation time of 60 fsec is, therefore, assumed. The final calculated result is shown in Fig. 5 which is in very good agreement with the corresponding experimental result reported in Ref. 1. If the damped oscillations reported in Refs. 1 and 2 are indeed due to the process discussed in this paper, the origins of the split levels 3 and 2 in the excited states, or similar split levels in the ground-state manifold, of the molecules studied remain to be determined.

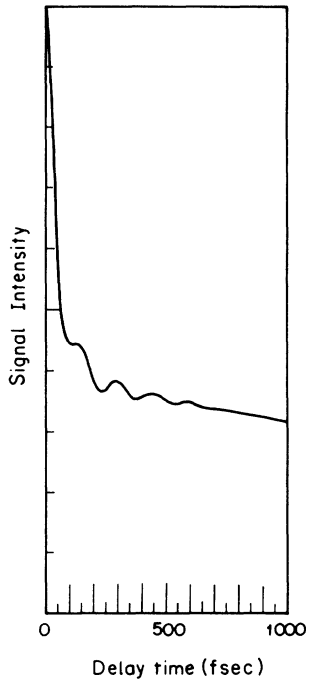

FIG. 5. Numerical simulation of the experimental transmission-correlation signal for malachite green reported in Ref. 1 based upon Eq. (10). $|p_{31}|/|p_{21}|=0.1$. The other parameters used in the calculation are given in the text.

III. CONCLUSIONS

In conclusion, the full density-matrix theory shows that quantum beats in optical transmission-correlation or pump-probe type of experiments can indeed be seen if the excitation pulses are short compared with the inverse line splitting between the sublevels in the excited state and the corresponding dephasing time. The beat pattern is essentially independent of the homogeneous or inhomogeneous broadening of the optical transitions. It is also found that the width of the coherent artifact in such measurements is not significantly affected by the homogeneous or inhomogeneous relaxation times of the optical transitions either. In fact, these types of measurements do not yield much useful information on the optical dephasing times T_2 or T_2^*.

We have carried out a similar theoretical analysis for the case using incoherent light; that is, when broadband incoherent light with a very short correlation time τ_c is used rather than short pulses of coherent light.[16] The theoretical approach developed in Sec. II is extended to this case in detail in the Appendix. Since incoherent light is regarded as a train of uncorrelated coherent pulses, quantum beats should be expected and the result of the Appendix shows that they are indeed observable by using incoherent light.

The theory can also be extended to the other type of three-level system: for example, if the split levels occur in the ground state rather than in the excited state, where the corresponding energy-level scheme is not different from that for conventional resonance Raman experiments. Transmission-correlation or pump-probe measurement is found to give quantum beats in this case also.

Note added in proof. Since the submission of this paper, two papers have been accepted for publication in the Comments section of Phys. Rev. Lett. confirming the interpretation that the observed oscillations in the transmission correlation is due to quantum beats have come to our attention: "Observation of Molecular Vibrations in Real Time" by J. Ha, M. Maris, W. Risen, J. Tauc, C. Thomsen, and Z. Vardeny of Brown University; and "Femtosecond Time-resolved Observation of Coherent Molecu-

lar Vibrational Motion" by K. Nelson and L. Williams of MIT.

ACKNOWLEDGMENTS

This work was completed when one of the authors (C.L.T.) was on leave at the Nippon Telegraph and Telephone Electrical Communications Laboratories in Musashino-shi, Japan. He would like to thank his colleagues in this laboratory for their hospitality and many stimulating discussions. His part of the work was supported in part by the National Science Foundation.

APPENDIX: INCOHERENT EXCITATION

Even when broadband incoherent light is employed in transmission-correlation measurements, the general result Eq. (8) is still applicable since the electric field $\mathscr{E}(t)$ was assumed to be arbitrary. The first or the second pulse amplitude $\epsilon(t)$ appearing in Eq. (9), however, is not a real smooth function but an ill-behaving complex function with correlation time τ_c, which is short compared to the real pulse width τ_p. Assuming $\epsilon(t)$ is complex, Eq. (10) can be rewritten as

$$
\begin{aligned}
S_{\mathrm{TC}}(\tau)=\frac{2\omega\rho_0}{\hbar^3}\mathscr{R}\int dt_4\int^{t_4}dt_3\int^{t_3}dt_2\int^{t_2}dt_1 e^{-(t_4-t_3+t_2-t_1)/T_2}
&\times[\epsilon(t_1)\epsilon^*(t_2)\epsilon(t_3-\tau)\epsilon^*(t_4-\tau)(N_++C_++B_+)\\
&+\epsilon^*(t_1)\epsilon(t_2)\epsilon(t_3-\tau)\epsilon^*(t_4-\tau)(N_-+C_-+B_-)\\
&+\epsilon(t_1-\tau)\epsilon^*(t_2-\tau)\epsilon(t_3)\epsilon^*(t_4)(N_++C_++B_+)\\
&+\epsilon^*(t_1-\tau)\epsilon(t_2-\tau)\epsilon(t_3)\epsilon^*(t_4)(N_-+C_-+B_-)\\
&+\epsilon(t_1)\epsilon^*(t_2-\tau)\epsilon(t_3-\tau)\epsilon^*(t_4)(N_++C_++B_+)\\
&+\epsilon(t_1-\tau)\epsilon^*(t_2)\epsilon(t_3)\epsilon^*(t_4-\tau)(N_++C_++B_+)\\
&+\epsilon^*(t_1)\epsilon(t_2-\tau)\epsilon(t_3)\epsilon^*(t_4-\tau)(N_-+C_-+B_-)\\
&+\epsilon^*(t_1-\tau)\epsilon(t_2)\epsilon(t_3-\tau)\epsilon^*(t_4)(N_-+C_-+B_-)]\,, \qquad \text{(A1)}
\end{aligned}
$$

where $N_\pm$, $B_\pm$, and $C_\pm$ are defined in Eq. (11).

For simplicity, we consider only the case of $T_2=0$. Then the above equation is greatly simplified since $t_1=t_2$, $t_3=t_4$, $N_+=N_-$, $B_+=B_-$, and $C_+=C_-$. By changing the variables $t_4\to t$ and $t_4-t_2\to s$, $S_{\mathrm{TC}}(\tau)$ is

$$
\begin{aligned}
S_{\mathrm{TC}}(\tau)\propto\int_0^\infty ds[(1+r^2)(e^{-\gamma s}+1)+2re^{-s/T_{2\mathrm{sub}}}\cos(\omega_{32}s)+2r]\\
\times\int_{-\infty}^{\infty}dt[\,|\epsilon(t-s)|^2|\epsilon(t-\tau)|^2+|\epsilon(t-s-\tau)|^2|\epsilon(t)|^2\\
+\epsilon(t-s)\epsilon^*(t-s-\tau)\epsilon^*(t)\epsilon(t-\tau)+\mathrm{c.c.}]\,, \qquad \text{(A2)}
\end{aligned}
$$

where $r=|p_{31}|^2/|p_{21}|^2$. This expression is similar to that obtained by Tomita and Matsuoka[16] but consists of the quantum-beat term. The first two terms of the second integral of Eq. (A2) has a sharp peak of width τ_p at $\tau=s$. Therefore, when τ_c is very small compared to γ^{-1}, $T_{2\mathrm{sub}}$, and ν_{32}^{-1}, the damped sinusoid appears as a function of τ in the final expression. This result assures the feasibility of observing quantum beats with incoherent light excitation.

[1]M. J. Rosker, F. W. Wise, and C. L. Tang, Phys. Rev. Lett. **57**, 321 (1986).

[2]F. W. Wise, M. J. Rosker, and C. L. Tang, J. Chem. Phys. (to be published).

[3]S. Haroche, J. A. Paisner, and A. L. Shawlaw, Phys. Rev. Lett. **30**, 948 (1973).

[4]W. R. Lambert, P. M. Felker, and A. H. Zewail, J. Chem. Phys. **75**, 5958 (1981).

[5]A. Corney and G. W. Series, Proc. Phys. Soc. London **83**, 207 (1964).

[6]J. N. Dodd, R. D. Kaul, and D. M. Warrington, Proc. Phys. Soc. London **84**, 176 (1964).

[7]D. J. Erskine, A. J. Taylor, and C. L. Tang, Appl. Phys. Lett. **45**, 54 (1984); A. J. Taylor, D. J. Erskine, and C. L. Tang, J. Opt. Soc. Am. B **2**, 663 (1984).

[8]E. P. Ippen and C. V. Shank, in *Ultrashort Light Pulses,* edited by S. Shapiro (Springer-Verlag, New York, 1977).

[9]Y. C. Chen, K. Chiang, and S. R. Hartmann, Phys. Rev. B **21**, 40 (1980).

[10]R. Beach and S. R. Hartmann, Phys. Rev. Lett. **53**, 663 (1984).

[11]H. Burggraf, M. Kuckartz, and H. Harde, in Proceeding of the International Quantum Electronics Conference, San Francisco, 1986 (unpublished).

[12]W. Lange and J. Mlynek, Phys. Rev. Lett. **40**, 1373 (1978); T. W. Ducas, M. G. Littman, and M. L. Zimmerman, *ibid.* **35**, 1752 (1975).

[13]J. E. Golub and T. W. Mossberg, in Proceeding of the International Quantum Electronics Conference, San Francisco, 1986 (unpublished).

[14]M. Mitsunaga and R. G. Brewer, Phys. Rev. A **32**, 1605 (1985).

[15]M. Mitsunaga, K. Kubodera, and H. Kanbe, Opt. Lett. **11**, 339 (1986).

[16]M. Tomita and M. Matsuoka, J. Opt. Soc. Am. B **3**, 560 (1986).